Tailoring the Metallocene Structure To Obtain LLDPE by Ethene Homopolymerization: An Experimental and Theoretical Study

Lucia Caporaso,* Nunzia Galdi, Leone Oliva, and Lorella Izzo*

Dipartimento di Chimica, Università di Salerno, 84084 Fisciano (SA), Italy

Received June 30, 2007

The mechanism of formation of branched polyethylene in the polymerization promoted by *meso*-metallocene/MAO systems has been investigated by combining DFT calculations and experimental results on differently featured *meso*-zirconocenes. A possible explanation for the required *meso* structure in the formation of branches considers a competition of ethene insertion and β-hydrogen transfer to the monomer. General mechanistic considerations in order to design catalytic systems able to synthesize LLDPE by ethene homopolymerization have been outlined.

1. Introduction

The synthesis of LLDPE by using ethene homopolymerization is industrially a challenge, considering that it is generally obtained by ethene copolymerization with 1-alkene. Within the *meso*-bis(indenyl)zirconocene family there are two classes, one producing high density polyethylene (HDPE) and the other affording linear low density polyethylene (LLDPE), with ethyl branches, in the ethene polymerization.[1–6] The presence and the amount of branches are the result of a balance between steric effects of substituent groups in the indenyl moieties and the kind of ligand bridge.[1–5] The analogous *meso*-titanocene and -hafnocene catalysts[6] as well as the more general *rac*-C_2-symmetric systems produce uniquely HDPE.[7]

Some of us found experimentally that the amount of ethyl branches in the LLDPE produced by *meso*-zirconocenes is independent of monomer concentration as well as counterion nature.[1,2,5] On the basis of this evidence, we hypothesized the mechanism for the branch formation.[1] Two diastereotopic active sites are present in the *meso*-like structure: the open one (defined as outward) and the encumbered one (defined as inward).[1,8] In our hypothesis, the formation of an ethyl branch in ethene polymerization is due to a β-hydrogen transfer from the growing chain to the monomer (BHT) coordinated at the outward site. Simultaneously the formation of a vinyl-terminated chain coordinated at the inward site and of an ethyl group σ -bonded to the metal takes place. Owing to the reinsertion of this macro-olefin into the M−ethyl bond, ethyl branch formation occurs. For the achievement of the whole mechanism the requirement should be a catalyst structure with a site where the growing chain can undergo the BHT reaction in competition with the olefin insertion (CP) (e.g., outward site) and a site in which the resulting macro-olefin coordinated to the metal does not dissociate but reinserts easily (e.g., inward site). These structural requirements are fulfilled by the *meso* configuration of the *ansa*-zirconocene.

In this paper we verify our hypothesis and we propose a more general correlation among ligand structure, β-hydrogen transfer to the monomer, and amount of ethyl branches by a combined experimental and theoretical study.

2. Results and Discussion

In order to rationalize the experimental data already reported in the literature, we performed calculations, with methods rooted in density functional theory (DFT), on ethene polymerization promoted by systems **1**−**7** in Chart 1 (for computational details see the Supporting Information). The internal energy differences of the transition states (TSs) for ethene insertion into the M−*n*-butyl chain (simulating the growing polymer chain) and β-hydrogen transfer from the *n*-butyl chain to the ethene ($\Delta E^{\ddagger}_{\mathrm{BHT\text{-}CP}}$)[9] were calculated for both inward and outward reactions.

As reported in Table 1, the $\Delta E^{\ddagger}_{\mathrm{BHT\text{-}CP}}$ values are positive, meaning that ethene insertion is always preferred at both sides. For system **1**, $\Delta E^{\ddagger}_{\mathrm{BHT\text{-}CP}}$ for the outward TSs is about 1.9 kcal/mol, and it increases up to 6.9 kcal/mol in the corresponding inward reaction. Since in our calculations the two BHT TS energies are almost the same for both sites,[10] the difference between the two $\Delta E^{\ddagger}_{\mathrm{BHT\text{-}CP}}$ values is clearly due to the lower insertion barrier (about 5 kcal/mol) of the inward CP TS with respect to the outward CP TS barrier.[11] This indicates insertion is favored on the inward site compared to the outward site.[12]

* To whom correspondence should be addressed. E-mail: lizzo@unisa.it (L.I.); lcaporaso@unisa.it.

(1) Izzo, L.; Caporaso, L.; Senatore, G.; Oliva, L. *Macromolecules* **1999**, *32*, 6913.

(2) Melillo, G.; Izzo, L.; Centore, R.; Tuzi, A.; Voskoboynikov, A. Z.; Oliva, L. *J. Mol. Catal. A: Chem.* **2005**, *230*, 29.

(3) Kokko, E.; Lhmus, P.; Leino, R.; Luttikhedde, J. G.; Ekholm, p.; Naesman, J. H.; Seppälä, J. V. *Macromolecules* **2000**, *33*, 9200.

(4) Izzo, L.; De Riccardis, F.; Alfano, C.; Caporaso, L.; Oliva, L. *Macromolecules* **2001**, *34*, 2.

(5) Izzo, L.; Puranen, A. J.; Repo, T.; Oliva L, *J. Polym. Sci., Part A: Polym. Chem.* **2006**, *44*, 3551.

(6) Melillo, G.; Izzo, L.; Zinna, M.; Tedesco, C.; Oliva, L. *Macromolecules* **2002**, *35*, 9256.

(7) See for example: (a) Brintzinger, H. H.; Fischer, D.; Mülhaupt, R.; Rieger, B.; Waymouth, R. M. *Angew. Chem., Int. Ed. Engl.* **1995**, *34*, 1143. (b) Resconi, L.; Cavallo, L.; Fait, A.; Piemontesi, F. *Chem. Rev.* **2000**, *100*, 1253. (c) Cobzaru, C.; Hild, S.; Boger, A.; Troll, C.; Rieger, B. *Coord. Chem. Rev.* **2006**, *250*, 189.

(8) Guerra, G.; Cavallo, L.; Moscardi, G.; Vacatello, M.; Corradini, P. *Macromolecules* **1996**, *29*, 4834.

(9) Since both CP and BHT originate from the same starting point, e.g. π-complex or counterion-bound M−alkyl species, we can directly compare the internal energy differences ($\Delta E^{\ddagger}_{\mathrm{BHT\text{-}CP}}$) of the TSs.

(10) The similar values can be easily explained on comparing Figure 1b with Figure 1d: the two BHT TS geometries differ in the position of the growing chain, the chains being too far from the metallocene skeleton and thus do not play any role in the relative TS energies.

10.1021/om7006562 CCC: $40.75
Publication on Web 03/06/2008

Chart 1. Systems Considered in This Study[a]

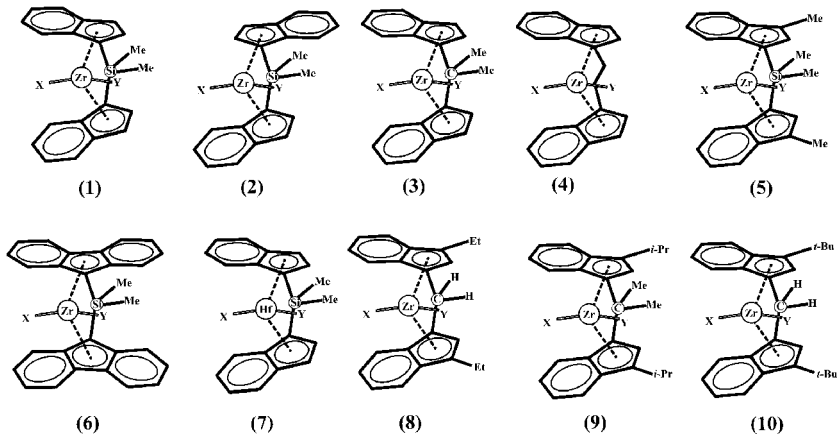

[a] X = *n*-butyl group and Y = ethylene in DFT calculations and X = Y = Cl in the experimental study.

Table 1. Theoretical and Experimental Results in the Ethene Polymerization Activated by Metallocene Catalytic Systems

	$\Delta E^{\ddagger}_{BHT\text{-}CP}$[a]		
system	inward	outward	ethyl branches[b] (mol %)
1	6.9	1.9	3.7
2	5.6	5.6	0
3	5.8	1.5	4.7[c]
4	7.8	3.6	
5	7.8	7.8	0[b]
6	9.5	4.6	0

[a] Internal energy differences ($\Delta E^{\ddagger}_{BHT\text{-}CP}$) in kcal/mol between the ethylene insertion transition state and the β-hydrogen transfer transition state. The values include ZPE correction.[13,17] [b] Referenced to polyethylenes obtained at 20 °C and at an ethylene feed concentration of 0.25 mol L^{-1}. The reported systems were activated with MAO. [c] System **3** gives double ethyl branches in addition to the ethyl branches.[4]

It is worth noting that the $\Delta E^{\ddagger}_{BHT\text{-}CP}$ value obtained for the analogous *rac*-system **2** is about 6.0 kcal/mol, close to the *inward* value obtained for the system **1**.

Calculations are in accordance with experimental data that show the *meso* system **1** is able to produce LLDPE with about 3.7% of ethyl branches,[2] while the *rac* form **2** leads to HDPE.[7] The experimental and theoretical data confirm and rationalize why the metallocene *meso* structure is required to obtain ethyl branches in the ethene homopolymerization: in the outward site the low $\Delta E^{\ddagger}_{BHT\text{-}CP}$ value allows the BHT reaction to compete with insertion and on the other hand the higher inward $\Delta E^{\ddagger}_{BHT\text{-}CP}$ value with a small insertion barrier makes possible an easy macro-olefin reinsertion. A general scheme is reported in Chart 2.

As reported in the literature, the compact CP four-center transition state requires a small space around the active metal with respect to the bulkier BHT six-center state and as a consequence, by closing the active pocket, the BHT TS is more

Chart 2. General Scheme of Formation of Ethyl Branches

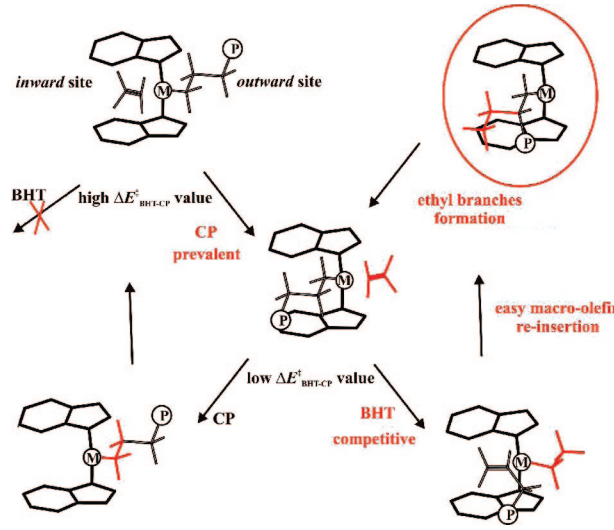

destabilized compared to the CP TS and vice versa.[13–15] It seems reasonable that $\Delta E^{\ddagger}_{BHT\text{-}CP}$ values can be tuned by varying the catalyst active pocket.

With this new picture in mind, we studied the behavior of the *meso* systems **1**−**7**, in order to verify the bridge, steric ligand hindrance, and metal atom effects on the $\Delta E^{\ddagger}_{BHT\text{-}CP}$ values and, as a consequence, on the branch formation.

Comparing the TS values obtained with the systems **1** and **3** (Table 1), one can observe that the C atom bridge in place of the Si opens the active pocket and as a consequence the $\Delta E^{\ddagger}_{BHT\text{-}CP}$ values decrease. An opposite trend in the $\Delta E^{\ddagger}_{BHT\text{-}CP}$ value is observed on going from system **1** to system **4** (Table 1), because the C_2H_4 bridge of system **4** compels the indenyl moieties in a

(11) The lower stability of the outward CP TS can be easily explained considering that the steric interactions between the growing chain and metallocenes skeleton forced the growing chain to move away from indenyl ligand (see the inward CP and outward CP TS geometries in Figure 1).

(12) A further confirmation of this conclusion is given by calculations performed on the two corresponding coordination intermediates, indicating that the inward coordination intermediate is less stable by about 4.0 kcal/mol with respect to the outward intermediate. This means that there is an outward CP barrier of about 9 kcal/mol but also an inward CP barrier of only 1 kcal/mol.

(13) (a) Talarico, G.; Blok, A. N. J.; Woo, T. K.; Cavallo, L. *Organometallics* **2002**, *21*, 4939. (b) Margl, P.; Deng, L.; Ziegler, T. *J. Am. Chem. Soc.* **1999**, *121*, 154–162. (c) Margl, P.; Deng, L.; Ziegler, T. *J. Am. Chem. Soc.* **1999**, *121*, 154–162. (d) Margl, P.; Deng, L.; Ziegler, T. *J. Am. Chem. Soc.* **1998**, *120*, 5517–5525. (e) Margl, P.; Deng, L.; Ziegler, T. *Organometallics* **1998**, *17*, 933–946.

(14) Talarico, G.; Busico, V.; Cavallo, L. *Organometallics* **2004**, *23*, 5989–5993.

(15) Deng, L.; Woo, T. K.; Cavallo, L.; Margel, P.; Ziegler, T. *J. Am. Chem. Soc.* **1997**, *119*, 6177.

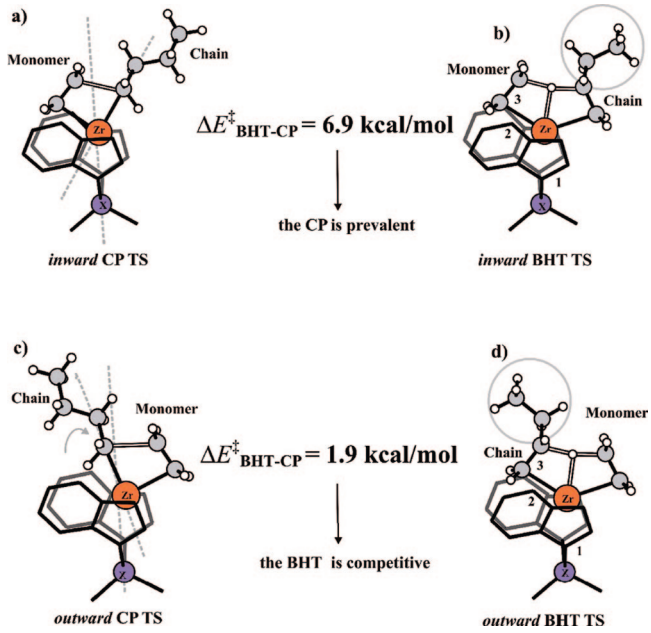

Figure 1. DFT transition state optimized structures for ethene insertion (left) and β-hydrogen transfer to the monomer (right) for the inward (**a** and **b**) and outward (**c** and **d**) sites. In each structure X is Si for system **1** and C for system **3**.

more hindered conformation.[16] The lower outward $\Delta E^{\ddagger}_{BHT\text{-}CP}$ value for system **3** and the higher outward $\Delta E^{\ddagger}_{BHT\text{-}CP}$ value for system **4** indicate a greater and a smaller tendency, respectively, to give β-hydrogen transfer to the monomer. Actually, system **3** produces polyethylene with both single and double ethyl branches, the latter attributed to a reiteration of the process after the formation of a single ethyl branch,[4] whereas the *meso*-$C_2H_4(Ind)_2ZrCl_2$ system (system **4**) is less efficient in the synthesis of branched polyethylene[1] (see Table 1). This agreement between calculations and experimental results points out that an open active pocket is advisable for producing LLDPE.

The *meso* systems **5** and **6** show the same inward site of the system **1** but a different hindrance in the outward one.[18] For these systems the outward $\Delta E^{\ddagger}_{BHT\text{-}CP}$ values increase on increasing the outward site hindrance. In fact, as reported in Figure 2, the two BHT TSs suffer more than the corresponding CP TSs of the repulsive steric interaction with the substituted metallocene skeleton.[19] These results seem to indicate that, upon encumbering the open site, the outward BHT barriers increase with respect to outward CP and the formation of the branches is prevented.

In order to verify experimentally the last statement, we synthesize and test new *meso* systems (**8** and **10** in Chart 1) in ethene polymerization. These systems show a gradual increase in the hindrance at the outward site with respect to the similar system **3**. After activation with methylalumoxane, they polymerize ethene to microstructurally different polymers (see Table 2). In fact, system **3**, characterized by the absence of substituents in 3,3′-positions of the bis(indenyl) ligand, produces LLDPE with about 2.6% of branches. System **8**, with ethyl substituent groups, is still able to produce branched polyethylene but with a lower content of branches (about 1.0%). Systems **9** and **10**, characterized by bulky substituents, isopropyl and *tert*-butyl groups, respectively, give linear polyethylenes. The amount of branches produced by system **3** increases up to 4.0% if one also considers the double ethyl branches not detected in the case of the other *meso*-zirconocene catalysts.

It is evident that the experimental results obtained with the aforementioned systems give us useful information on the outward site influence on the polyethylene microstructure. Considering that in ^{13}C NMR spectra of polymers obtained with the most bulky systems **9** and **10** neither ethyl branches nor vinyl chain ends were detected, it seems reasonable to conclude that when the encumbrance of the indenyl substituents is increased, the outward $\Delta E^{\ddagger}_{BHT\text{-}CP}$ values increase and consequently the formation of linear polyethylene is favored. This trend is in accordance with experimental data already reported for system **6**, where the encumbrance is due to the presence of a C6-ring condensed to the indenyl ring, and it is well explained by the above-reported calculations.

A last remark concerns the role of the metal on the *meso*-metallocene systems on branch formation. We have already reported that *meso*-titanocene and -hafnocene catalysts produce linear polyethylene without a detectable amount of branches.[6] This evidence can be accommodated in the framework of our mechanism, considering that Ti is smaller than Zr and consequently the active pocket is more closed. From such simple considerations, it is reasonable to expect a high value for $\Delta E^{\ddagger}_{BHT\text{-}CP}$ of the outward position that prevents the β-hydrogen transfer. On the other hand, in the literature there are also reports as a general trend of the higher aptitude of the Hf catalytic systems toward chain propagation with respect to the BHT reaction, in comparison with the analogous Zr catalytic system reaction.[13b,20] We calculated the outward $\Delta E^{\ddagger}_{BHT\text{-}CP}$ on the Hf-based system **7** (Table 1) as 4.6 kcal/mol, which is higher than the corresponding Zr value. This justifies why system **7** is not able to produce LLDPE by ethene homopolymerization.

3. Conclusions

In this paper, our hypothesis concerning the mechanism of branch formation has been verified through computational analysis and further experimental evidence. By using DFT calculations and by tuning experimentally the ligand framework, we demonstrated that the mechanism of branched polyethylene formation involves a catalytic system with two diastereotopic sites, one characterized by a small energy difference between β-hydrogen transfer to the monomer and monomer insertion ($\Delta E^{\ddagger}_{BHT\text{-}CP}$ value) and the other by a higher $\Delta E^{\ddagger}_{BHT\text{-}CP}$ value. When β-hydrogen transfer to the monomer (BHT) occurs in the outward site, the macro-olefin reinsertion in the inward site allows the formation of ethyl branches in the polymer chain. In this respect, the role of the ligand framework such as a bridge,

(16) The energy differences of the $\Delta E^{\ddagger}_{BHT\text{-}CP}$ values can be attributed to the C2−C3 distances, which are 3.4 Å in system **1**, 3.5 Å in system **3** (see Figure 1b,d), and 3.3 Å in system **4**.

(17) The calculated $\Delta E^{\ddagger}_{BHT\text{-}CP}$ values reported in Table 1 do not include solvent and counterion effects; therefore, they cannot be expected to confirm the absolute experimental percentage of branches in the polyethylene samples. However, they can be used reliably to extract trends, because the aforementioned effects can be safely assumed to be similar when comparing similar reaction profiles.

(18) Since it is already known that alkyl substitution on the 2,2′-indenyl positions reduces the effect of the metallocene systems toward BHT, we investigated the effect of the substitution on 3,3′-positions on branch formation. We also analyzed the bis(fluorenyl) system because it shows the same hindrance at the sites.

(19) For system **5**, the monomer is the same distance from the methyl carbon substituent in the TS of both competitive processes (see C5−C4 distances in Figure 2a,b), while the distance between the growing chain and the methyl carbon substituent is shorter in BHT with respect to the corresponding CP (see C2−C3 distances in Figure 2a,b). For system **6**, the six-center BHT has a shorter distance to both the monomer and growing chain with respect to the corresponding CP (compare C4−C5 and C2−C3 distances in Figure 2c,d).

(20) Heiland, K.; Kaminsky, W. *Makromol. Chem.* **1992**, *193*, 601.

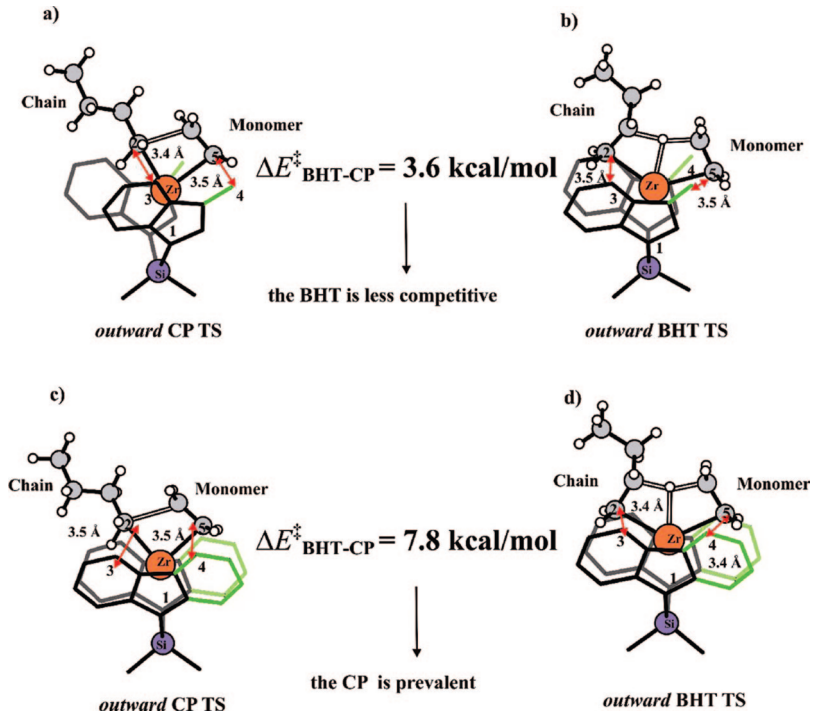

Figure 2. DFT transition state optimized structures for ethene insertion (left) and for outward β-hydrogen transfer to the monomer (right) of systems **5** (**a** and **b**, respectively) and **6** (**c** and **d**, respectively).

Table 2. Percentage of Ethyl Branches and Melting Temperatures of Polyethylenes Obtained in the Presence of *meso* Systems with a Single Carbon Atom Bridge, Activated by MAO at Different Polymerization Temperatures and Ethylene Feed Composition

system	groups in C(3,3′)	T (°C)	P_{ethene} (atm)	$[E]_{feed}$ (mol L^{-1})	ethyl branches[a] (%)	T_m (°C)	M_n
3	−H	50	6	1.1	3.0	121	1.0×10^3
		50	1	0.16	0.6	121	2.1×10^3
		20	1	0.25	1.8	120	0.9×10^3
		0	1	0.35	2.8	118	2.6×10^3
		−20	1	0.50	2.0	127	n.d.
8	$-CH_2CH_3$	50	5	1.1	0.7	128	4.1×10^4
		50	1	0.16	1.0	126	4.7×10^4
		20	1	0.25	0.8	128	4.5×10^4
9	$-CH(CH_3)_2$	50	1	0.16	n.d.	130	1.7×10^5
		20	1	0.25	n.d.	133	1.2×10^5
		0	1	0.35	n.d.	132	1.5×10^5
		−20	1	0.50	n.d.	130	9.0×10^4
10	$-C(CH_3)_3$	50	5	0.87	n.d.	134	1.9×10^5
		50	1	0.16	n.d.	132	1.0×10^5
		20	1	0.25	n.d.	131	1.2×10^5
		0	1	0.35	n.d.	133	1.3×10^5
		−20	1	0.50	n.d.	133	1.3×10^5

[a] Calculated by ^{13}C NMR spectra from the relative intensity of a branch methylene carbon and an inner chain carbon.

as well as the substituents, or the metal has been clarified through the full accordance between experimental and theoretical results.

Our conclusion might be useful for the rational design of new catalytic systems active in the LLDPE synthesis by ethene homopolymerization, and we are currently extending these analyses to catalytic systems with a ligand framework different from that of the *meso*-zirconocene catalysts.

4. Experimental Section

All manipulations involving air-sensitive compounds were carried out under nitrogen atmosphere using Schlenk or drybox techniques. Toluene was dried over sodium and distilled before use. MAO, purchased from Witco as 10% solution in toluene, was dried to be used as a powdery white solid. Polymerization grade ethene was purchased from SON and further purified by bubbling through a 5 mol % xylene solution of Al^iBu_3.

4.1. Synthesis of Catalyst Precursors. *meso*-$Me_2C(Ind)_2ZrCl_2$, *meso*-$Me_2C(3\text{-}i\text{-}Pr\text{-}Ind)_2ZrCl_2$, and *meso*-$CH_2(3\text{-}t\text{-}Bu\text{-}Ind)_2ZrCl_2$ were synthesized according to the literature procedure[21] and characterized by ^1H NMR.

Synthesis of Bis(1-ethyl-3-indenyl)methane. A 3.6 mL amount of formalin (37% solution, 48.6 mmol) was added dropwise to a mixture of ethylindene (97 mmol) and sodium ethoxide in 140 mL of dimethylformamide. The reaction mixture was stirred for 18 h at room temperature, and then 1 M HCl (120 mL) was added and the organic layer was extracted with petroleum ether (3 × 100 mL).

(21) (a) Resconi, L.; Balboni, D.; Baruzzi, G.; Fiori, C.; Guidotti, S. *Organometallics* **2000**, *19*, 420–429. (b) Izzo, L.; Napoli, M.; Oliva, L. *Macromolecules* **2003**, *36*, 9340–9345. (c) Spaleck, W.; Antberg, M.; Dolle, V.; Klein, R.; Rohrmann, J.; Winter, A. *New J. Chem.* **1990**, *14*, 499.

The organic layers were collected, dried over Na_2SO_4, and concentrated. The ligand was purified through chromatography (yield 20%).

^{1}H NMR ($CDCl_3$): δ 7.47–7.23 (m, 8H, C_6H_4); 6.21 (d, 2H, C_5 ring =CH); 3.75 (s, 2H, CH_2 bridge); 3.05 (m, 2H, C_5 ring, CH); 1.55 (m, 4H, CH_2); 0.91 (s, 6H, CH_3).

Synthesis of Bis[3-ethyl-3-(trimethylstannyl)indenyl]methane. To a solution of bis(1-ethyl-3-indenyl)methane (8.8 mmol) in 45 mL of diethyl ether was added, dropwise, at −78 °C, *n*BuLi (2.5 M solution in hexane, 17.6 mmol). The mixture was stirred for 1 h at −78 °C, warmed to room temperature, and stirred for 18 h. After that, the solution was treated at −40 °C with Me_3SnCl (18 mmol) in 5 mL of diethyl ether and stirred overnight. The solvent was evaporated to yield an orange oil (mixture of *syn* and *anti* isomers; yield 70%).

^{1}H NMR ($CDCl_3$): δ 7.48–7.16 (m, 8H, C_6H_4); 6.36 (s, 2H, C_5 ring, CH); 2.25 (s, 2H, CH_2 bridge); 1.56 (m, 4H, CH_2); 0.87 (t, 6H, CH_3); −0.11 (s, 18H, $Sn(CH_3)_3$).

Synthesis of *meso*-CH_2(3,3′-ethyl-bis(indenyl))zirconium Dichloride. A solution of bis[3-ethyl-3-(trimethylstannyl)indenyl]-methane (6.5 mmol) in 10 mL of toluene was added dropwise to a suspension of $ZrCl_4$ (6.5 mmol) in 22 mL of toluene. The mixture was stirred for 18 h at room temperature and then for 4 h at 100 °C. The *meso* form was separated from the *rac* form through crystallization from fresh, dry toluene (the *meso* form is more soluble than the *rac* form). (yield 45% based on ligand).

^{1}H NMR ($CDCl_3$): δ 7.49–6.91 (m, 8H, C_6H_4); 5.57 (s, 2H, C_5 ring, CH); 5.05 (d, 1H, CH_2 bridge); 4.76 (d, 1H, CH_2 bridge); 2.82 (m, 4H, CH_2); 1.19 (t, 6H, CH_3).

4.2. Ethene Polymerization. Polymerizations were carried out in a 100 mL glass flask equipped with a magnetic stirrer or in a 250 mL stirred glass autoclave. Toluene (20 or 150 mL), powdered MAO (mol of Al/mol of Zr = 1000), and 5.6 μmol of catalyst precursor were added under a nitrogen atmosphere, the flask was thermostated at the desired temperature, evacuated, and filled with ethene. The polymerization mixtures were then poured into acidified ethanol. The quenched polymers were recovered by filtration and dried under reduced pressure at 80 °C.

Activity (g of polymer/((mg of Zr) h $[E]_{feed}$)): 0.02−1.8 (systems **3** and **8**); 2.1−3.4 (systems **9** and **10**).

Ethene composition in the liquid phase was calculated by Lewis and Luke's equation and using the fugacity function chart.[22]

4.3. Polymer Analysis. ^{13}C NMR spectra were recorded on a Bruker Advance 300 MHz spectrometer at 373 K with D1 = 4 s, and the chemical shifts are referenced to the central peak of 1,1,2,2-tetrachloroethane-d_2 ($C_2D_2Cl_4$) used as internal reference at δ 72.16 ppm.

Melting points were measured using a Du Pont 2920 differential scanning calorimeter with a heating rate of 10 °C/min on about 10 mg of sample.

GPCs were recorded on a Waters 150-C gel-permeation chromatograph with four polystyrene gel columns (10^4 Å pore size) in dichlorobenzene at 120 °C and calibrated with polystyrene.

4.4. Computational Details. DFT quantum-mechanics calculations were performed with Gaussian03,[23] using the B3LYP functional[24] and the LANL2DZ basis and ECP on the metal atom[25] and the SVP basis set on all other atoms.[13a,26] Minima were localized by full optimization of the starting structures, while the transition states for the insertion reaction were approached through a linear transit procedure starting from the olefin-coordinated intermediate and then located by a full transition state search. In our model the growing chain is simulate with *n*-butyl group according with literature.[13a]

Acknowledgment. We thank Dr. Patrizia Oliva (University of Salerno) for technical assistance for the NMR analyses. This work was financially supported by Regione Campania (L.R. 5/2002).

Supporting Information Available: Tables and text giving Cartesian coordinates, energy values, and single negative frequencies of all the structures and computational details. This material is available free of charge via the Internet at http://pubs.acs.org.

OM7006562

(22) (a) Lewis, W. K.; Luke, C. D. *Trans. Am. Soc. Mech. Eng.* **1932**, 54–55. (b) Maxwell, J. B. *Data Book on Hydrocarbons*; Van Nostrand: New York, 1950.

(23) Frisch, J.; Trucks, G. W.; Schlegel, H. B.; Scuseria, G. E.; Robb, M. A.; Cheeseman, J. R.; Montgomery, Jr., J.A.; Vreven, T.; Kudin, K. N.; Burant, J. C.; Millam, J. M.; Iyengar, S. S.; Tomasi, J.; Barone, V.; Mennucci, B.; Cossi, M.; Scalmani, G.; Rega, N.; Petersson, G. A.; Nakatsuji, H.; Hada, M.; Ehara, M.; Toyota, K.; Fukuda, R.; Hasegawa, J.; Ishida, M.; Nakajima, T.; Honda, Y.; Kitao, O.; Nakai, H.; Klene, M.; Li, X.; Knox, J. E.; Hratchian, H. P.; Cross, J. B.; Bakken, V.; Adamo, C.; Jaramillo, J.; Gomperts, R.; Stratmann, R. E.; Yazyev, O.; ustin, A. J.; Cammi, R.; Pomelli, C.; Ochterski, J. W.; Ayala, P. Y.; Morokuma, K.; Voth, G. A.; Salvador, P.; Dannenberg, J. J.; Zakrzewski, V. G.; Dapprich, S.; Daniels, A. D.; Strain, M. C.; Farkas, O.; Malick, D. K.; Rabuck, A. D.; Raghavachari, K.; Foresman, J. B.; Ortiz, J. V.; Cui, Q.; Baboul, A. G.; Clifford, S.; Cioslowski, J.; Stefanov, B. B.; Liu, G.; Liashenko, A.; Piskorz, P.; Komaromi, I.; Martin, R. L.; Fox, D. J.; Keith, T.; Al-Laham, M. A.; Peng, C. Y.; Nanayakkara, A.; Challacombe, M.; Gill, P. M. W.; Johnson, B.; Chen, W.; Wong, M. W.; Gonzalez, C.; Pople, J. A. Gaussian 03, Revision C.02; Gaussian, Inc., Wallingford CT, 2004.

(24) (a) Lee, C.; Yang, W.; Parr, R. G. *Phys. Rev. B* **1988**, *37*, 785. (b) Becke, A. D. *J. Chem. Phys.* **1993**, *98*, 1372. (c) Becke, A. D. *J. Chem. Phys.* **1993**, *98*, 5648.

(25) (a) Dunning T. H., Jr.; Hay, P. J. In *Modern Theoretical Chemistry*; Schaefer, H. F., III, Ed.; Plenum: New York, 1976; Vol. 3, pp 1–28. (b) Hay, P. J.; Wadt, W. R. *J. Chem. Phys.* **1985**, *82*, 270. (c) Wadt, W. R.; Hay, P. J. *J. Chem. Phys.* **1985**, *82*, 284. (d) Hay, P. J.; Wadt, W. R. *J. Chem. Phys.* **1985**, *82*, 299.

(26) Schäfer, A.; Horn, H.; Ahlrichs, R. *J. Chem. Phys.* **1992**, *97*, 2571.